Covariances and Linear Predictability of the Atlantic Ocean

Carl Wunsch
Room 54-1426
Department of Earth, Atmospheric and Planetary Sciences,
Massachusetts Institute of Technology
Cambridge MA 02139 USA
email: cwunsch@mit.edu, Tel: 1-617-253-5937

August 23, 2011

Abstract

The problem of understanding linear predictability of elements of the ocean circulation is explored in the Atlantic Ocean for two disparate elements: (1) sea surface temperature (SST) under the storm track in a small region east of the Grand Banks and, (2) the meridional overturning circulation north of 30.5°S. To be worthwhile, any nonlinear method would need to exhibit greater skill, and so a rough baseline from which to judge more complex methods is the goal. A 16-year ocean state estimate is used, under the assumption that internal oceanic variability is dominating externally imposed changes. Linear predictability is the story of time and space correlations, and some predictive skill exists for a few months in SST, with some minor capability extending to a few years. Sixteen years is, however, *far too short* for an evaluation for interannual, much less decadal, variability, although orders of magnitude are likely stably estimated. The meridional structure of the meridional overturning circulation (MOC), defined as the time-varying vertical integral to the maximum meridional volume transport at each latitude, shows nearly complete decorrelation in the variability across about 35°N—the Gulf Stream system. If a time scale exists displaying coherence of the MOC between sub-polar and subtropical gyres, it lies beyond the existing observation duration, and that has consequences for observing system strategies and the more general problem of detectability of change.

1 Introduction

The ability to predict future climate is high on the agenda of many scientists (e.g., Meehl et al., 2009; Hurrell et al., 2010; Mehta et al., 2011). Claims that climate should be predictable on some time-scale often rest upon the assumption that it would arise from the long memory of the ocean—the atmosphere being assumed to lack such memory.

At the present time, more specifically, there is wide community interest in the possibility of decadal prediction of some elements of the ocean circulation, including sea level changes (e.g., Yin et al., 2009), surface temperatures (Newman, 2007), and volume transports (Zhang and Wu, 2010; Msadek et al., 2010). Government funding agencies have issued calls for actual forecasts to be made (see e.g., the websites of the US National Science Foundation and of the European Science Foundation). The comparatively short decadal time-scale raises the possibility of observational tests of actual predictions, something that is implausible with 50 to 100 year forecasts—durations which exceed working scientific lifetimes, of model credibility, and the interval since about 1992 of global-scale ocean observations. The extent, however, of actual predictive skill for the ocean even on the decadal time-scale, much less the multi-decadal one, remains obscure, with divergences of IPCC model extrapolations being a disquieting sign. Some models are undoubtedly better than others, but which those are, and which fields are well-calculated, remains unknown. Branstator and Teng (2010) review much of the existing discussion.

Almost all studies of oceanic and its potential in climate predictability have been based upon model calculations, and these have generally led to optimistic inferences (e.g., Msadek et al., 2010). Some modelling studies have, however, led to more cautious conclusions. For example Bingham et al. (2007) found little decadal meridional correlation between large-scale transport characteristics—implying that any predictive skill in one region would have little impact on larger scale, climatically important, components. In a study of the impact of noise disturbances on the meridional overturning circulation (MOC), Zanna et al. (2011) found, for an idealized configuration, that so-called non-normal error growth, particularly from small changes at depth in sub-polar regions, would limit MOC predictive skill to considerably less than one decade.

In broader terms, predictability of the changes of any physical system involves several sub-elements, including: the extent to which boundary conditions are predictable; the degree to which variations arise from internal fluctuations with fixed or known boundary conditions; and the degree to which that internal variability is fundamentally linear or non-linear. In particular, any discussion of oceanic predictability confronts the awkward fact that the ocean tends to react, rapidly and energetically, to shifts in the overlying atmosphere, particularly to changes in the wind-field, most visibly in its upper reaches and often with little or no spatial correlation. (The most rapid response is the barotropic one, which is almost instantaneous over the whole water column.) A literature has emerged showing the coupling of the North Atlantic circulation to the North Atlantic Oscillation (NAO, or Arctic Oscillation, AO) index; see e.g., Deser et al.

(2010). Some of the most important elements of the ocean circulation, as they affect climate, such as the sea ice cover, or sea surface temperature (SST) are greatly modified by changing wind systems, and they in turn, modify the atmosphere. This inference directs attention to the more central question of whether the *atmosphere* is predictable on decadal time scales. No discussion is provided of the probability that externally imposed finite amplitude shifts will occur, such as the catastrophic collapse of the West Antarctic Ice Sheet (WAIS) and its numerous consequences.

The purpose of this paper is to explore some of the simpler aspects of the ocean prediction problem employing, primarily, observations. The focus is on changes that are assumed, absent strong evidence to the contrary, as arising from intrinsic ocean variability, rather than that induced by global warming or other external drivers. Because there exist so many possible predictable elements, we arbitrarily focus first on sea surface temperature (SST), and then on the meridional overturning circulation (MOC) as exemplary of many of the issues. Attention shifts to the most stable components embodied in the oceanic baroclinic structure. Simple theory (Veronis and Stommel, 1956; Anderson et al., 1979) shows that, short of catastrophic external disturbances, and outside of the equatorial band, basic characteristics such as the thermocline depth and temperatures can be modified significantly only over many decades.

Notwithstanding several claims for the existence of major shifts in the ocean circulation, there is *no* observational evidence in historical times of observed changes in basin-scale or larger basic oceanic stratification or transport properties that lie beyond what are best labelled "perturbations" and for which linearization about a background state is a useful starting assumption. One can compare e.g., the RRS Challenger (Tizard et al., 1873) hydrographic section, New York to Puerto Rico, to recent sections nearby—without detecting any qualitative change. Rossby et al. (2010) note that no detectable shift in mid-latitude Gulf Stream properties has occurred over the last 80 years. It does remain possible that comparatively small changes in e.g., sea surface temperature or sea ice cover, can generate major regional or global atmospheric climate shifts—but if the oceanic component can be treated as essentially one of linear dynamics, a substantially simplified oceanographic problem is the result.

The onset or suppression of such small spatial scale phenomena as rates, regions, and water mass properties of convective regions are almost surely important to prediction skill over long times as water mass production slowly accumulates. Convection and related processes would generally have a nonlinear component—as they depend upon threshold-crossing physics. Whether any existing nonlinear ocean model can reliably forecast such shifts is unknown. In any case, Gebbie and Huybers (2011) show that surface sources of abyssal ocean waters are far more widely distributed geographically than is conventionally believed.

If the perturbation depiction has any merit, it leads to the question of whether there is any *linear* forecast skill. If the answer is "yes", then any nonlinear approach e.g., through particle filters, large ensembles, or simple runout of the of underlying GCM would have to exhibit a significantly increased skill-level relative to the linear ones to justify the added expense. If the answer is "no," that there is no linear skill, one is led to understand how the nonlinear system might be able, nonetheless, to produce a significant improvement. In any case, as for most problems, it is worth exploring linear approximations before moving on to more complex forms.

Theoretical prediction skill is not meaningful unless it is coupled with a discussion of the ability to detect it. Thus for example, a prediction that the meridional overturning circulation will weaken by 1 Sv in 10 years might be correct, but if neither the present nor the future values can be determined to that accuracy, at best one could say that the future value will not be distinguishable from the present one. Observational detection accuracy is a function of the scope and nature of the observation system, and of the structure of the variability noise in the ocean. Although it is touched on only tangentially here and is rarely discussed elsewhere, this issue of *detectability* is an essential ingredient in any useful discussion of forecast skill—and deserves study in its own right. A closely related, also rarely discussed, question has already been alluded to: what magnitude of change could be regarded as useful, for example, in producing a measurable contribution to future climate shifts?

In proceeding, another difficult question concerns those elements one is trying to predict, and why? Myriad choices are phenomenological (sea surface temperature, sea level, meridional overturning,....), geographical (western North Atlantic, tropical eastern Pacific), seasonal (winter time SST versus summer time), and time horizon (SST with a one month lead time can be of intense interest to a weather forecaster, while the MOC state may be of interest only on 100+ year scales and then only to scientists). Here two fields of interest to different communities (North Atlantic SST and the Atlantic MOC), are chosen, simplified as far as possible, and the methodologies sketched that can be applied in seeking more definitive answers.

Linear predictability is the story of correlations of fields in space and time and thus their estimates come to play the central role here. The observation-oriented approach, given the extremely limited duration of large-scale oceanic observations relative to a multi-decadal requirement, leads to the inference that one can hardly do more than state the problem. Resort to models can and is being made, but the same data duration limitations preclude real model tests.

2 An Ocean State Estimate

To proceed as best we can, the ocean state estimate ECCO-GODAE, v3.73, is used. This estimate is discussed in detail by Wunsch and Heimbach (2007), Wunsch et al. (2009), and in other papers listed on the website, http://www.ecco-group.org. For present purposes, a sufficient description is that this state estimate is a near-global one over 16 years, from a least-squares fit using Lagrange multipliers to the comparatively large oceanographic data sets that became available beginning about 1992 in the World Ocean Circulation Experiment and later. Adjustable parameters include initial conditions and all of the meteorological forcing functions. The solution used is from this adjusted, and freely running, model. A partial discussion of the time-mean of the estimate can be found in Wunsch (2011); the character of that mean relative to dynamical equilibrium does have implications for predictability, and which will be touched on at the end.

A terminology, "state estimate," is used here to distinguish the result from estimates based upon versions of meteorological forecast techniques ("data assimilation")—which lead to products with physically impossible jumps and without global conservation principles. The results here are primarily governed by observations, distinguishing them from the pure model runs: Over the vast bulk of the oceans, the estimate is in a slowly time-evolving, volume and heat-salt-conserving, thermal-wind balance, largely constrained by in situ hydrography, Argo float profiles, and altimetric variability. It is thus a best-fit geostrophic, hydrostatic balance, in which absolute velocities are determined from the conservation equations subject to Ekman pumping and other surface forcing. Note that, among other data sets, monthly estimates of SST by Reynolds and Smith (1995) were used.

Sixteen years is an extremely short period over which to determine multi-year or decadal predictive skill. The restriction to that time period is dictated by the extreme paucity of oceanic data prior to about 1992—when WOCE was underway. Ocean state estimates over intervals before 1992 (e.g., Wang et al., 2010) are from nearly unconstrained ocean models. Furthermore, the meteorological forcing fields used, even the most recent ones, have known major errors; see e.g., Bengtsson et al. (2004) or Bromwich et al. (2007).

Because of the short-duration, a comparison will be made to the longer interval (28 years) Reynolds and Smith (1995; hereafter RS) SST estimate used, separately, without the intervening ECCO system. Such estimates are, however, not available for other fields of interest (the meridional overturning, the corresponding oceanic heat transports, etc.), and for them the state estimates must be used. The even-longer historical reconstructions of SST obtained prior to the arrival of globally orbiting satellites are also avoided here, as the space-time sampling errors are far worse.

3 Sea Surface Temperature (SST)

SST is always of central interest to meteorologists and provides a convenient starting point for this investigation despite its being one of the most volatile and complex of all oceanic fields. Vinogradova et al. (2010) discuss the global behavior of SST (particularly its rate of change) in the ECCO solutions. Fig. 1 displays the time-mean SST over the 16-year duration of the ECCO estimate

Woollings et al. (2010) have discussed elements of atmospheric storm track behavior resulting from greatly increasing the SST resolution in the Gulf Stream region—where dominant atmospheric cyclogenesis is thought to be most pronounced. The 1° version of the ECCO model does not have sufficient resolution to reproduce the details of the Gulf Stream south of New England, but it does do a reasonable job further north and east—in the sense of producing an acceptable misfit to the data. Here the initial region of generic discussion is the small area east of the Grand Banks depicted in Fig. 1, and which is close to being the eastern half of the Woollings et al. (2010) region of interest. For the area (which will be referred to as the "Grand Banks Box" or GBB, and denoted with a subscript G), the spatial average, $T_G(t)$, is formed and is plotted in Fig. 2. The present focus on a small region contrasts with the notable effort by Davis (1976) directed at the largest-scale features in the Pacific Ocean.

The time average of $T_G(t)$ is $\langle T_G(t)\rangle = 9.6 \pm 3.2°\text{C}$. A simple, and perhaps even useful, prediction of the temperature is its mean. In the present case, the annual cycle is so visually apparent (not true of most oceanographic variables), that one is immediately led to a discussion of its predictability. To the degree that it is purely periodic, one can extrapolate indefinitely into the future. On the other hand, every seasonal cycle differs at least slightly from every other one, and hence predictive skill will be imperfect. Fig. 3 displays the periodogram of $T_G(t)$, showing that the annual cycle typically has about 90% of the variance over 16 years, with a smaller contribution from the semiannual and higher harmonics. At this resolution, there is a sharp peak at the annual period, of bandwidth less than the resolution limit of 1 cycle/16 years, meaning that it is indistinguishable from a pure sinusoid. Note, however, that the background energy surrounding and under this peak is not negligible and this energy prevents perfect prediction of that component. (Methods exist, not necessary here, for predicting slowly changing annual cycles; e.g., Hannan, 1970).

Using least-squares, the annual cycle and its first three harmonics were removed from the record, leaving a residual, $T'_G(t)$, shown in Fig. 4, and producing an annual cycle amplitude of $4.3 \pm 0.23°$C (the error is the formal one from the least-squares residuals). The variance of the complete record is $10.2°\mathrm{C}^2$, of which the deterministic annual cycle (and three overtones) accounts for $9.4°\mathrm{C}^2$ or 93% (see Table 1). Variance dominance by the annual cycle is a challenge to any model attempting to calculate either it, or the small deviations from it—should its details change with climate. Of the residual 7%, most (about 5% of the total variance) lies in periods longer than one year. Discussion of prediction now requires separating the problems at interannual and intra-seasonal time scales.

3.1 A Formalism

With the removal of the annual cycle and its harmonics, as well as the time-mean, the residual time series, $T'_G(t)$, can be assumed indistinguishable from a weakly stationary random process.[1] Many techniques exist for their prediction, and the literature is extremely large. Useful summaries can be found in Robinson (1981), Hamilton (1994), Nelles (2001), Box et al. (2008), von Storch and Zwiers (2001), and Priestley (1982, Ch. 10) among many others. General developments are associated with the names of Wold, Kolmogoroff, Wiener, Levinson etc., but the most common formulation is through the development of autoregressive models of order N (AR(N)), moving averages of order M (MA(M)), and combined models (ARMA(N,M)), and their generalizations to non-stationary and nonlinear processes. Davis (1976, 1978, 1979) provides excellent summaries of climate applications.

These linear methods, when new, were applied with a notable lack of success to ordinary weather and stock market prediction. With understanding of the chaotic nature of weather, the result is unsurprising. Rumors do persist that significant amounts of money can be made using these methods in the stockmarket over minutes to hour time-scales, but on longer times the stockmarket is not a stationary linear system. The present effort thus could be a quixotic one—except that the degree to which, and which elements of the ocean circulation are chaotic on decadal time scales, remains unknown. In any case, as argued above, there is little evidence of large-scale deviations from slight perturbations in the observed circulation, and linearity is a plausible starting point.

Here we will use primarily the AR and MA formulations (briefly summarized in Appendix A) although the calculations are done in a slightly unorthodox manner to more directly emphasize the underdetermined nature of the problem. Consider any zero-mean time series variable, $\xi(t)$, which initially will be $T'_G(t)$. Suppose, to provide a specific example, that there exist L

[1] Weak, or wide-sense, stationarity requires that the mean and second moments of the time series should be time-independent.

observations, including the present, and that it is an AR(2) process,

$$\xi(t) = a_1\xi(t-1) + a_2\xi(t-2) + \varepsilon(t), \tag{1}$$ {ar3}

where a_1, a_2 are unknown regression constants and $\varepsilon(t)$ is near-Gaussian white noise of zero mean and variance σ_ε^2. Unless otherwise stipulated, t, denotes the present time, and the time-steps, Δt are implicit in all expressions. The coefficients in Eqs. (1) are in practice a set of simultaneous equations for the unknown $a_1, a_2, \varepsilon(r)$,

$$\begin{aligned}
\xi(t) &= a_1\xi(t-1) + a_2\xi(t-2) + \varepsilon(t) \\
\xi(t-1) &= a_1\xi(t-2) + a_2\xi(t-3) + \varepsilon(t-1) \\
\xi(t-2) &= a_1\xi(t-3) + a_2\xi(t-4) + \varepsilon(t-2) \\
&. \\
&. \\
\xi(t-(L-3)) &= a_1\xi(t-(L-2)) + a_2\xi(t-(L-1)) + \varepsilon(t-(L-3)),
\end{aligned} \tag{2}$$ {ar4}

for $L-2$ equations in L unknowns (a_1, a_2, and $L-2$ of the $\varepsilon(r)$). Re-write Eq. (2) in standard matrix vector notation as,

$$\mathbf{Ex} = \mathbf{y}, \quad \mathbf{E} = \left\{ \begin{array}{cccccccc}
\xi(t-1) & \xi(t-2) & 1 & 0 & . & 0 & 0 \\
\xi(t-2) & \xi(t-3) & 0 & 1 & . & 0 & 0 \\
. & . & 0 & 0 & . & 0 & 0 \\
. & . & . & . & . & . & . \\
\xi(t-(L-2)) & \xi(t-(L-1)) & 0 & 0 & . & 0 & 1
\end{array} \right\}, \tag{3}$$ {ls2}

$$\mathbf{x} = \begin{bmatrix} a_1 \\ a_2 \\ \varepsilon(t) \\ \varepsilon(t-1) \\ . \\ \varepsilon(t-(L-3)) \end{bmatrix}, \; \mathbf{y} = \begin{bmatrix} \xi(t) \\ \xi(t-1) \\ \xi(t-2) \\ . \\ . \\ \xi(t-(L-3)) \end{bmatrix},$$

a formally underdetermined problem and which can be solved in numerous ways, including those commonly used in regression problems (e.g., Box et al., 2008; Priestley, 1982). The present formulation as a set of simultaneous equations differs from conventional least-squares (Priestley, 1982, P. 346) only in treating the $\varepsilon(r)$ as explicitly part of the solution, rather than as residuals of the formally over-determined problem for a_1, a_2 alone. Here, for several reasons, we choose this depiction (Wunsch, 2006): the formal regression problem, when many more physical variables are reasonably introduced (e.g., the SST time series at all latitudes, or the wind field), rapidly becomes very underdetermined even in the conventional formulation; least-squares makes simple the computation of uncertainties in the parameters $(a_1, a_2, \varepsilon(r))$; and one can easily "color" the noise $\varepsilon(t)$ either by modification of the identity matrix appearing in $\mathbf{E}$ (which would make it an ARMA), or by introducing column weighting (solution covariance) matrices. Extension to arbitrary order AR processes is readily carried out. The normal equations governing the least-squares solutions of Eq. (3) involve the sample autocovariances of the ξ, known as the Yule-Walker equations.

For convenience in prediction, it is helpful to know that any stationary univariate AR can be converted into an MA, of form,

$$\xi(t) = \sum_{p=0}^{\infty} b_p \varepsilon(t-p) = \varepsilon(t) + b_1 \varepsilon(t-1) + b_2 \varepsilon(t-2) + \ldots \tag{4}$$

{ma1}

For known a_i, the b_i can be obtained by algebraic long division,

$$1 + b_1 z + b_2 z^2 + \ldots = \frac{1}{1 + a_1 z + a_2 z^2 + a_3 z^3 + \ldots}, \tag{5}$$

{zpoly}

and vice-versa. The b_i can also be determined directly without first calculating the a_i. The MA form produces the $\tau-$ahead *prediction error* (PE) as,

$$\left\langle \left(\tilde{\xi}(t+\tau) - \xi(\tau+\tau) \right)^2 \right\rangle = \sigma_\varepsilon^2 \sum_{p=0}^{\tau} b_p^2, \quad b_0 = 1, \tag{6}$$

{pe1}

the tilde denoting the prediction. This equation is obtained by substituting $\xi(t+\tau)$ into the left-hand-side of Eq. (6) and replacing the unknown and unpredictable $\varepsilon(t+1), \ldots, \epsilon(t+\tau)$ by their zero-means. If the b_i are sufficiently small, there will be rapid convergence to the asymptote of the variance of $\xi(r)$: $\langle \xi^2 \rangle = \sigma_\varepsilon^2 \sum_{p=0}^{\infty} b_p^2$. Like an $N-$order AR, any practical MA will have a finite order, M. Generally speaking if M is small, N will be large, and vice-versa, and with the trade-off becoming part of the discussion of representational efficiency. Note that stationarity, which we are assuming, requires that the polynomials in Eq. (5) should both be convergent when $|z| = 1$ (they are "minimum phase" in the signal processing terminology). Prediction error cannot exceed the variance of the time series—linear prediction cannot produce an error exceeding that from using the mean value.

Linear predictive skill for processes having a known power density spectrum can be determined either by first computing the corresponding autocovariance and proceeding directly to the Yule-Walker equations, or more elegantly by using the Wiener-Kolmogoroff spectral factorization method (see Robinson, 1959, P. 105, or Priestley, 1982, Ch. 10). The spectral approach shows explicitly the connection between linear predictive power and the degree of frequency structure.

A time series with a flat (white) spectrum is unpredictable at any lead-time, τ, except for its mean value; structured spectra, including generic red noise, correspond to some additional linear predictive capability; and line spectra (pure periodicities) have infinite predictive time horizons. Many time series in nature are a mixture of these and other characteristics, and the fraction of the total variance that is predictable, and over what lead time, depends upon the details of the spectrum.

4 Months-Ahead Prediction

This autoregressive machinery is now used to estimate how predictable is $T'_G(t)$ (Fig. 4) about its mean, when sampled at monthly intervals? The red spectrum (an approximately -2.5 power law) of the residual (Fig. 3) shows that there is some predictability, dominated by the lowest frequencies. Because monthly and interannual physics are likely to be distinct, the question will be attempted in two stages: monthly mean samples and monthly forecasting and, annual mean samples and annual forecasting.

Because the solution to Eqs. (3) produces the same result as the conventional methods, standard statistical tests (e.g., Ljung, 1999; Priestley, 1982) can be used to infer that $T'_G(t)$ can be represented as an autoregressive process with order between 3 and 6 (the tests differ). Because an AR(3) captures almost as much of the variance as do the higher order models, and is the simplest, we choose that as a reference case. The result, from solving the least-squares problem is,

$$T'_G(t+1) = 0.92\,(0.71)\,T(t) - 0.29\,(0.1)\,T(t-1) + 0.22\,(0.07)\,T(t-2) + \varepsilon(t+1)\,, \quad \Delta t = 1\text{month},$$

where the parenthetical number is the standard error, with $\tilde{\sigma}_\varepsilon^2 = 0.2°\mathrm{C}^2$.

Directly estimating the MA form produces, alternatively,

$$T'_G(t) = 1.0\varepsilon(t) + 0.92\varepsilon(t-1) + 0.556\varepsilon(t-2) + 0.465\varepsilon(t-3) + 0.469\varepsilon(t-4) + ...,$$

and which is slowly convergent. These MA forms were used to calculate the prediction error, which grows month-by-month (Fig. 5, Table 1) ultimately asymptoting after about 8 or 9 months to the full variance of $T'_G(t)$. (Recall that the total variance after removal of the annual cycle and its overtones is about $0.7°\mathrm{C}^2$—and represents the maximum prediction error relative to the mean.) One might reasonably infer that there is useful (at the level of a few tenths of a degree error) linear predictive skill out to 4 or 5 months in the future, but not much beyond. Whether such skill is useful would depend upon the purpose of the prediction.

4.1 Comparison to the Satellite Record

Using the Reynolds and Smith (1995; RS) fields from this area, one can extend a similar SST record out to 28 years. Details are not shown here, but a summary statement is that while the monthly results differ in detail from those found for the ECCO-estimated record, there is no qualitative difference, except that the apparent trend is more conspicuously reversing in recent years (Fig. 6 and Table 1).

5 Interannual Behavior

Interannual behavior of the record is highly problematic: 16 samples (annual means) is far too short to make much of any inference about correlation and prediction ability. The textbooks already cited show how to calculate standard error statistics for the AR or MA coefficients, a_i, b_i, etc., and which depend directly on the autocovariances—assuming roughly Gaussian behavior. To make the issue concrete, however, a small ensemble example for an AR(1)—the structure with the fewest possible parameters other than white noise—is displayed in Appendix B and the instability of the estimates from such small samples is obvious. We proceed here by restricting the representation to an AR(1)—with the results interpreted cautiously as indicative only of orders of magnitude.

5.1 Predicting Annual Averages of $T'_G(t)$

Fig. 6 shows the annual averages, $\bar{T}'_G(t)$, of the residuals of $T'_G(t)$ for both the state estimate and the RS values. The state estimate shows a visible trend and a zero-order puzzle is the question of whether that trend is a true secular one induced by global warming (defined here as extending uniformly far beyond the record length), or a mere low frequency fluctuation manifested by red noise (see Wunsch, 2010, for more discussion of the difficulties of trend determination, and further references). Here it will arbitrarily be assumed that this signature is indeed a component of red noise, as the longer RS record suggests, and thus will contribute to the predictive skill of the interannual signal.

The one-year-ahead prediction error is approximately $0.03°\mathrm{C}^2$ rising to $0.2°\mathrm{C}^2$ after about 4 years (see Fig. 7 and Table 1). If a linear trend is first removed, neither the order nor thepredicti on error (PE) are changed significantly. The RS results, not discussed, are very similar. All that should be inferred is that linear predictive methods suggest some skill out to about 5 years with errors of a few tenths of a degree. Whether any more sophisticated system can do better remains, as of this writing, unknown.

5.2 Predictability—A Caveat

The reader is reminded that this study is based upon a "hindcast" skill, meaning that the same data are used to determine the time series structure as are used to test its prediction skill. Hindcast skill is inflated relative to true forecast skill by a significant amount. Davis (1976) has a clear discussion of the issue. As he notes, an accurate estimate of the skill inflation is only simple with large-sample statistics and, in particular, for interannual behavior, the estimated SST used here is a very small sample. It is useful, in many cases, to withhold part of the data set as a way of emulating an independent record for testing skill, perhaps by dividing it into two pieces—an identification section and a test section. But the "red" nature of the spectra observed shows that there will exist significant correlations between the used and withheld portions of the time series, and again a rigorous calculation becomes difficult. We leave the discussion at this point—as a warning that estimates here, particularly of the interannual forecast skill, are optimistic ones.

6 The Meridional Overturning Circulation (MOC)

That the Atlantic MOC has become the center of so many studies, theoretical and observational, is largely the result of the propagation of "conveyor belt" or "ribbon" pictures of the circulation, whatever their physical reality might be. The MOC does provide a rough measure of the intensity of the circulation in data and models. MOC connection to climate variability is, however, at best indirect, and determining the volume or mass transport in the North Atlantic as a whole can be done only by use of a model. A number of papers (e.g., Lorbacher et al., 2010) claim the existence of useful covariances between MOC values and some observables such as sea surface height, except these are also untested model results. Another immediate issue is the definition of what is meant by the MOC, as the literature contains usages calculating it at very different latitudes, integration depths, and averaging times. Here we take advantage of a global system to define it—in the Atlantic Ocean—as a function of all latitudes from the Cape of Good Hope (about 30°S) northward to the northern limits of the present model (79.5°N). It is, more specifically, calculated as the zonal integral at monthly intervals, continent to continent, of the meridional velocity, the density being treated as constant, consistent here with the Boussinesq version of the model,

$$V\left(y,z,t\right)=\int_{0}^{x_L(y)} v\left(x,y,z,t\right)dx \qquad (7)$$ {meridtrans1}

(in practice, spherical coordinates are used). At any latitude, at any time, the MOC is then arbitrarily defined as the maximum of the integral from the surface to a time and space varying depth $z_{\max}(y)$,

$$V_{moc}(y,t) = \max_{z_{\max}(y,t)} \int_{z_{\max}(y,t)}^{0} V(y,z,t)\, dz \tag{8}$$

Fig. 8 displays the time average value, $\langle V_{moc}(y,t)\rangle$ as well as the depth, $z_{\max}$, where, on average, the maximum is reached (Fig. 9) . A geographical maximum of about 16Sv is reached at northern mid-latitudes and drops rapidly with latitude beyond about 50°N. At the present time, it is not possible to provide a useful uncertainty estimate for these values, but the general structure—mass-conserving thermal wind-balance—appears very robust to both variations in the data base and in model parameters. The meridional flows, V, were discussed in some detail by Wunsch and Heimbach (2006, 2009).

How much does $V(y,z,t)$ vary with time? Jayne and Marotzke (2001) infer, consistent with what is found here, that the seasonal volume variability arises primarily in the surface Ekman layer. Fig. 10 shows the meridional transport January anomaly values every two years, indicating variations of up to about 4Sv, but only very locally—mainly in the vicinity of the equator, and at about 40°N. The variations in the anomaly of $V_{moc}(y,t)$ are shown in Fig. 11 at three latitudes, where the integration depth is kept fixed at $z_{moc}(y)$, that is not time-varying. These integrals have a range, except in the far north, of about ±5Sv and are noisy on monthly time scales. Temporal variances of V at all latitudes are depicted in Fig. 12. The power densities for three latitudes are shown in Fig. 13. At most latitudes, there is a significant annual cycle and its harmonics, especially in the low-latitude Ekman layer. Otherwise, the spectral densities are nearly white beyond the annual period—boding ill for decadal linear predictability. The smallest low frequency energy is found at 50.5°N, a result consistent with the linear dynamical behavior there requiring much longer adjustment times. High latitude power densities are dominated by the annual cycle and not by the interannual variability (out to 16 years). In general, these spectra are "flat" by geophysical standards, being not very far from white noise.

Variances of the MOC, computed for the monthly means over all 111 latitudes are $27\text{Sv}^2 = (5.1\text{Sv})^2$ and the annual means have variance $1.5\text{Sv}^2 = (1.2\text{Sv})^2$ providing a rough idea of the temporal variability and the observational challenge. At 50.5°N alone, the corresponding variances are $10.5\text{Sv}^2 = (3.2\text{Sv})^2$, and $1.8\text{Sv}^2 = (1.3\text{Sv})^2$.

A small visible trend appears early on in the values at some latitudes, a trend which disappears as one moves away from the starting time. No data precede the start time of 1992; hence the early years are much more weakly constrained than the later ones—which are controlled in considerable part by the data preceding the particular time of estimation.

Fig. 14 shows the correlation coefficient matrix, R_{ij}, between the annual mean variations in the MOC at all latitudes, i, j. Making the mildly optimistic assumption that each of the annual mean values is an independent variable at any latitude, at 95% confidence, one must have $|R_{ij}| > 0.5$, approximately, to distinguish the value from zero. A change takes place across about 35.5°N where all linear correlation is lost between values on either side of that latitude (the approximate Gulf Stream position). The North Atlantic subtropical gyre shows some marginally significant correlation with the South Atlantic, but no correlation with the North Atlantic subpolar gyre (consistent e.g., with the pure model results of Bingham et al., 2007) except for a slight hint of a finite relationship between 75°N and the South Atlantic. Within the subtropical gyre, correlation decays to insignificant levels beyond separations of about 20°of latitude. (A more elaborate analysis by E. Haam, personal communication, 2011, using a Monte Carlo simulation (Haam and Huybers, 2010), suggests that the small band of higher correlation between about 75°N and the South Atlantic, visible as horizontal and vertical stripes in Fig. 14, is statistically significant. An oceanic physical mechanism for "skipping over" the intermediate latitudes is not obvious, and one probably must look to the atmosphere for an explanation.)

A problem with correlation analyses is that they lump together all time scales, often having very diverse physics. One might hypothesize that the low correlations found here are the result of noisy high frequencies. To address this issue in part, Figs. 15 and 16 show the coherence as a function of frequency between the 50.5°N MOC and its values at 25.5°N and 20.5°S. They show, to the contrary, that the only marginal coherence is at periods shorter than one year (at the annual period the conventional statistics do not apply as sinusoids are always coherent). Evidently (on this decadal time scale), annual mean MOC determinations south of about 35°N carry no (linear) information about its behavior poleward of that latitude at any frequency now testable.

One could search the system for correlations. For example, it is conceivable that there is correlation between the meridional transports lying between some pair of isopycnals, at two different latitudes, even though the total transport shows nothing significant. If one searches a large number of possible combinations, some apparently significant relationship will necessarily be found. If there are 100 possible combinations, then using a 95% level-of-no-significance with proper probability densities, about 5% should show apparent, but spurious, correlation. This direction is not pursued.

6.1 Predicting the MOC

Monthly predictions of the MOC have no obvious utility and they are not discussed here; only the annual means are now considered. Wunsch and Heimbach (2009) discuss the annual cycle of the MOC—and which is primarily a near-equatorial phenomenon, extending to considerable depth. Hypothetically, one could imagine using each of the 111 time series at 1° latitude spacing, with time lags of one year and longer, as regression variables to predict e.g., the value at some specific latitude(s). With 16 sample points at any fixed latitude, one would be seeking the equivalent of the expansion of a 16-dimensional vector in 111 non-orthogonal vectors—as in Appendix C—a markedly underdetermined problem. Although we will return to this problem, consider instead the more well-determined one of predicting from the present and past values at one particular latitude. As for SST, the main problem is having only 16 samples,

The MOC at 50.5°N is arbitrarily chosen as the initial target prediction—on the basis of a large literature claiming that modifications in the high latitude transports are a key climate control parameter. This latitude is close to the one with the largest defined MOC and is just south of the region where the mean MOC declines very rapidly. Thus consider the problem of predicting the MOC at 50.5°N one year into the future, using the calculated history at that latitude. The spectral estimate in Fig. 13 is not very different from white noise at long periods, and one anticipates only some modest degree of prediction skill. Fig. 17 shows the error growth using an AR(1) deduced from the measurements at 50.5°N alone (and see Table 1).

Had there appeared significant correlations or coherences between 50.5°N and other latitudes, it would be reasonable to seek predictive power from observed variations in the MOC at all latitudes. The absence of such correlations shows that linear predictability will be slight. Experiments using singular vectors (not shown; Appendix C describes them), as expected did not produce any useful outcome.

It is, of course, possible that the existing 16-year interval is untypical of the longer-term behavior of the Atlantic Ocean and/or that linear predictive skill would emerge with much longer, multi-decadal or centenary, records, but these are purely speculative claims. The utility for prediction from existing duration, geographically widely separated, field observations is doubtful.

6.2 Correlation with SST

Study of the MOC has often been justified on the basis that its variability is linked to climate change, sometimes in truly dramatic fashion ("hosing" and "shut-down"). Thus the question arises as to whether there is any relationship between the MOC variations estimated here, and the SST of the region previously discussed. One simple measure is the correlation coefficient between the MOC and GBB SST variations, depicted in Fig. 18, which repeats Fig. 14, but such that the last row and column now represent the annual mean SST time series. The calculation is shown for the case of the raw SST and where, also, its visible, linear, trend was removed by least-squares. One might infer that there is a marginally significant negative correlation between the low latitude MOC ($0 \pm 10°$ latitude) and the GBB SST. The result is, however, dependent upon the presence of the trend in SST, and which destroys the assumption of annually independent changes. Any inference of correlation is extremely fragile and not supportive of a relationship between MOC and SST on the time scales accessible here. Determining whether there is such a relationship on much longer time scales will have to wait on extended observations.

7 Discussion

Linear predictability in space-time systems is the story of the covariance structure. It is thus useful to compare the results for the MOC here with the entirely different approach and inferences of Msadek et al. (2010) as an example of a pure model approach. They concluded that the MOC is predictable with some skill out to 20 years, using an unconstrained, coupled climate model run for 1600 years. Apart from the very much longer analysis time, their mean MOC is 25 Sv rather than the approximate maximum of 16 Sv found here. Their MOC spectrum (their Fig. 1) is steeply red from about two year periods to about 20 years, culminating in a narrow-band spectral peak near 20 years. That their inferred predictability is larger than found here, at about 20 years, would be a consequence of their narrow spectral peak at that period—if it is real. This prediction skill is likely primarily a linear one, because low frequency narrow-band processes have an intrinsic long memory—extended correlation times; as the peak-width becomes narrower, one converges to a deterministic component with an infinite prediction horizon. In contrast, the spectra computed here tend to indicate a white noise behavior beyond about 15-year periods with no indication of a narrow band spectral process, although no definitive statement can be made from the available observations.

This disagreement between the two sets of results focuses one on the central conundrum of climate change studies: (1) It is difficult to compare a 16-year data-constrained estimate to a 1600-year unconstrained one. (In their study of 136 years of North Atlantic SST data, Tourre et al. (1999) did not report any obvious 20 year spectral excess, although all the caveats about data quality before the polar-orbiting satellite era will apply, and even that recent system is imperfect.) Conceivably, the present 16-year interval of the ECCO estimates is unrepresentative e.g., of the historical strength of the MOC, and one might postulate that it was more typically closer to the 25Sv of the Msadek et al. (2010) model than to the ECCO values of the WOCE era. Such an enhanced value, however, would imply a much increased geostrophic transport, which dominates the upper limb of the MOC —mostly in the Gulf Stream system. Within historical times, such a large strength is probably ruled out by existing coastal sea level and wind-strength records, but no quantitative estimate has been made. (2) Conceivably the more nearly white spectrum that we infer at periods of a few years is also untypical of a hypothetical much longer record. How does one know?

A general comment, applicable also to the present results, is that most models are much less noisy than is the real world, either entirely lacking in the eddy field and internal waves, or commonly underestimating them. In the present case (e.g., Wunsch, 2008; Kanzow et al., 2009) and in calculations such as Msadek et al. (2010), one should infer that all estimates of predictability (or its relative, detectability) skill are probably upper bounds.

Poor prediction results in the fields discussed here does *not* mean that the corresponding variable is not predictable: sometimes the best prediction is just the sample mean, with a standard error given from the variance of the variable. That is, given observing system limitations, and the great oceanic noisiness, the best prediction may well be that the field will be indistinguishable from present values—and that estimate may still be a useful one. A nonlinear method, one that was independent of any linear space-time correlation, might well do better, although the nonlinearity would have to be one operating on statistical moments higher than the second. Note that methods exist for transforming some nonlinear time series into linear forms (e.g., Hamilton, 1994, etc.).

One can modify and extend the methods here in a large number of ways. The singular value decomposition (see Appendix C) is identical in its $\mathbf{u}$ vectors to the conventionally defined EOFs, and emerges naturally as part of the least-squares/regression problem. These individual orthogonal structures of the variability have been used by Davis (1978) and many others. Generally speaking, any particular EOF (singular vector) will have a fraction, depending upon the degree of spatial correlation, of the total variance, and if it displays significant predictability (e.g., Branstator and Teng, 2010), it will only be for that fraction of the expected variance—perhaps large enough to be useful to someone if its skill can be tested.

The dual (adjoint) model calculations of Heimbach et al. (2011) represent a running linearization of the governing equations about the time-varying state. Regarded as Green function solutions, they can be used either directly in predictions, or as a guide in choosing the relevant regressor fields, locations, and time-scales. They do show the strong sensitivity of North Atlantic shifts to disturbances in distant ocean basins at earlier times. On time scales of decades and longer, variability in the Atlantic is a summation of disturbances emanating from the entire global ocean. No single region dominates the later changes in the North Atlantic, and for understanding and prediction, a global, long-duration observing system is required.

As noted in the Introduction, the present results apply only to the temporally statistically stationary components. A major shift in the controlling boundary conditions—such as a massive ice melt event, or an increase in greenhouse gases—would render the process non-stationary—changing its mean, and likely its higher statistical moments as well. The issue for those interested in decadal and longer predictability is whether those external controls are predictable and whether they dominate the variance contributed by what here is assumed to be intrinsic changes in the ocean. Such external predictability, if it exists, is primarily independent of purely oceanic processes and their long memory components. A long memory has the consequence, however, of producing changes today or in the future as the result of forcings and fluctuations occurring long ago (Heimbach et al., 2011), greatly complicating the interpretation of ongoing changes.

The results here have all been biased towards an optimistic outcome: using the estimated fields both to determine the optimal linear predictors and to test them; usually retaining apparent trends; and by employing very large scale integrals such as basin-wide transports. Consistent with the earlier study of the linear predictability of the North Atlantic Oscillation (NAO; Wunsch, 1999), little skill beyond a year is found. Major elements of the ocean circulation are of course, predictable far beyond that time interval: it is a very safe prediction that the thermocline depth, the net heat content, etc. will be little changed in a decade or longer, probably undetectably so, given the nature of the observing system and the natural noise.

In their comparison of three different model calculations of the Atlantic MOC, Bingham et al. (2007) drew conclusions that are broadly similar to those found here, albeit differing in the details. They found essentially no correlation in their three models between the MOC in the subpolar and subtropical gyres, but did succeed in identifying a weak (relative to the overall variability) lowest singular vector (EOF) representing a coupling of the two. The duration of observations required to detect it was not estimated, but would clearly be extremely long compared to any existing records.

Lack of correlation seen between the subtropical and subpolar regions can be understood in rather simple terms: as discussed e.g., in Wunsch (2011) for the same state estimate, the dynamical time scales for adjustment of disturbances grows very rapidly with latitude beyond about 40°, so that finding simple lag correlations between gyres would be very surprising. Over 16 years, the subtropical gyre was found to be in near equilibrium with the wind forcing, while subpolar regions were not—consistent with the time-scale growth.

Climate change is a global phenomenon, integrating at any given location changes originating from diverse regions of the globe, not just locally, and the spatially de-correlating local responses represent a summation over all times and space. If there is a timescale beyond which the MOC shows large meridional coherences and/or coherence with SST as in the conveyor "ribbon" cartoons, it appears to lie beyond the duration of any existing record. Sustenance over many decades (Rossby et al., 2005, is an example) of globally distributed, top-to-bottom, observations is urgently required, although a "hard-sell."

Acknowledgments. Written in honor of Tom Rossby—a true pioneer of the observed-ocean. Supported in part by ECCO-GODAE and the North Atlantic Meridional Overturning Circulation Program (both NASA-funded) and our many partners in that effort. Thanks to C. King and D. Spiegel for help with the model output and data sets. Comments from P. Huybers, R. E. Davis, P. Heimbach, and the very detailed suggestions of two referees are appreciated.

Appendix A. The Vector Least-Squares Approach to Prediction

Scalar Time Series

Much of the conceptual underpinning of the standard regression methods can be simplified through a vector-least-squares point of view. The advantage is that least-squares permits a very general, and flexible, method to deal with, among other problems, the underdetermined problem of more regressors than regressees, and introduces the empirical orthogonal functions (EOFs) naturally via the singular value decomposition. Nothing that follows is original, but is a heuristic description of discrete stationary time series as discussed in innumerable textbooks.

Consider a stochastic zero-mean anomaly, $\xi\left(t=t_{now}\right)$, where t_{now} represents the instant in time when the value of ξ is known, as are its past values, and one seeks to predict its future behavior. The time scale is chosen so that the interval is $\Delta t=1$. Form a vector from $\xi\left(t\right)$ as

$$\boldsymbol{\xi}\left(t\right)=\left[...\xi(t-q),\xi(t-q+1),...,\xi(t-1),\xi(t)\right]^T$$

that is constructed from its formally infinite past and terminating at $t=t_{now}$. Let L be the actual number of observed elements, including the one at the present time. Superscript T denotes the transpose in the convention that, unless otherwise stated, all vectors have column form. Define a second vector in which everything is shifted to the right, dropping the most recent value,

$$\boldsymbol{\xi}\left(t-1\right)=\left[...\xi(t-q),\xi(t-q+1),...,\xi(t-2),\xi(t-1)\right]^T$$

—and which of necessity, in practice will have only $L-1$ non-zero elements. The collection of all such vectors, $\boldsymbol{\xi}\left(t-p\right)=\left[...\xi(t-q),\xi(t-q+1),...,\xi(t-p-1),\xi(t-p)\right]^T$ is a generally non-orthogonal set, noting that in observational practice the last one, $\boldsymbol{\xi}\left(L\right)$, will have only one non-zero element. This, and other, observed long-lagged vectors will thus be poor approximations to the theoretically defined semi-infinite vector.

Now consider another formally defined vector derived from $\xi(t)$, $\xi\left(t+\tau\right)$ as a semi-infinite one, $\tau>0$,

$$\boldsymbol{\xi}\left(t+\tau\right)=\left[...\xi\left(t+\tau-q\right),...,\xi\left(t+\tau-1\right),\xi\left(t+\tau\right)\right]^T,$$

that is displaced in the opposite time direction relative to $\xi\left(t\right)$ and including the unknown *future* values

$$\xi\left(t+1\right),\xi\left(t+2\right),...,\xi\left(t+\tau\right).$$

$\boldsymbol{\xi}\left(t+\tau\right)$ is just another vector, and unless it is orthogonal to the collection of known past vectors, $\boldsymbol{\xi}\left(t-p\right),p\geq 0$, one should be able to at least partially represent it in those non-orthogonal vectors,

$$\boldsymbol{\xi}\left(t+\tau\right)= \tag{9}$$
$$\alpha\left(\tau\right)\boldsymbol{\xi}\left(t\right)+\alpha\left(\tau+1\right)\boldsymbol{\xi}\left(t-1\right)+...+\alpha\left(\tau+K\right)\boldsymbol{\xi}\left(t-K\right)+\boldsymbol{\varepsilon}\left(t+\tau\right),\quad K\leq L-1.$$

{vector1}

The $\alpha\left(\tau\right)$ are simply the coefficients of the vector expansion, and for a stationary process would depend only upon τ, and not t. $\varepsilon\left(t+\tau\right)$ is an error representing any elements of $\boldsymbol{\xi}\left(t+\tau\right)$ that are orthogonal to the expansion vectors (and which are the $\tau-$lead-time "prediction error"). Determining how far back into the past, $t-K$, one should carry Eq. (9) is an important part of the inferential process. Clearly as K approaches L, the number of zero elements in the expansion vectors grows, and the particular $\boldsymbol{\xi}\left(t-K\right)$ will be a poor representation of the true vector. One prefers, $K << L$. Similarly, physical insight comes into the discussion, as Eq. (9) is a finite difference equation and will typically be an approximation to some partial differential system describing the time (and space) evolution of the elements $\boldsymbol{\xi}\left(t+\tau\right)$.

The simplest case is $K=1$, and $\tau=1$, and writing it out in full, one has,

$$\left\{\begin{array}{c}\xi\left(t-1\right)\\ \xi\left(t-2\right)\\ .\\ .\\ \xi\left(t-\left(L-1\right)\right)\end{array}\right\}a_1+\left[\begin{array}{c}\varepsilon\left(t\right)\\ \varepsilon\left(t-1\right)\\ .\\ .\\ \varepsilon\left(t-\left(L-2\right)\right)\end{array}\right]=\left[\begin{array}{c}\xi\left(t\right)\\ \xi\left(t-1\right)\\ .\\ .\\ \xi\left(t-\left(L-2\right)\right)\end{array}\right]. \tag{10}$$

{vector2}

$$\text{or,}\quad \mathbf{E}_1\mathbf{x}+\boldsymbol{\varepsilon}=\mathbf{d},\ \mathbf{x}=a_1, \tag{11}$$

The maximum number of equations is $L-1$, involving the past data as far back as $\xi\left(t-\left(L-1\right)\right)$.

An alternative formulation is Eq. (3) in the text:

$$\mathbf{E}\mathbf{x}=\mathbf{y},\quad \mathbf{E}=\left\{\begin{array}{cccccc}\xi\left(t-1\right) & 1 & 0 & . & 0 & 0\\ \xi\left(t-2\right) & 0 & 1 & . & 0 & 0\\ . & 0 & 0 & . & 0 & 0\\ . & . & . & . & . & .\\ \xi\left(t-\left(L-1\right)\right) & 0 & 0 & . & 0 & 1\end{array}\right\}, \tag{12}$$

$$\mathbf{x}=\left[\begin{array}{c}a_1\\ \varepsilon\left(t\right)\\ \varepsilon\left(t-1\right)\\ .\\ \varepsilon\left(t-\left(L-2\right)\right)\end{array}\right],\ \mathbf{y}=\left[\begin{array}{c}\xi\left(t\right)\\ \xi\left(t-1\right)\\ \xi\left(t-2\right)\\ .\\ .\\ \xi\left(t-\left(L-2\right)\right)\end{array}\right],$$

which identifies the values of $\varepsilon(r)$ as explicit unknowns. Now $\mathbf{E} = \{\mathbf{E}_1 | \mathbf{I}\}$.

The conventional least-squares solution is (e.g., Wunsch, 2006),

$$\begin{aligned}\tilde{\mathbf{x}} = \tilde{a}_1 &= \left(\mathbf{E}_1^T \mathbf{E}_1\right)^{-1} \mathbf{E}_1^T \mathbf{d} \\ &= \frac{1/L \sum_{q=0}^{L-2} \xi(t-q-1)\,\xi(t-q)}{1/L \sum_{q=0}^{L-2} \xi(t-q-1)^2}\end{aligned} \tag{13}$$

{ls1}

which minimizes $\tilde{\boldsymbol{\varepsilon}}^T \tilde{\boldsymbol{\varepsilon}}$. The one-step prediction error (PE) is, $\tilde{\varepsilon} = \mathbf{d} - \mathbf{E}_1 \tilde{\mathbf{x}}$. The tildes are used as a reminder that the solution is an estimate. As in any other least-squares problem, one must test the residuals, $\tilde{\boldsymbol{\varepsilon}}$**,** for a white-noise character. If $\tilde{\boldsymbol{\varepsilon}}$ passes that test, it is described simply by its variance, σ_ε^2. Ordinary least-squares (e.g., Lawson and Hanson, 1995; Wunsch, 2006) produces estimates of the expected error in $\tilde{\mathbf{x}}$, etc. Quantities such as $(1/L) \sum_{q=1}^{L-1} \xi(t-q+1)\,\xi(t-q)$ in Eq. (13) are the empirical autocovariances of $\xi(t)$ and the most conventional approach to these problems (e.g., Box et al., 2008; Priestley, 1982) formulates the problem explicitly by invoking the covariances—which are the dot (inner) products of the expansion vectors in the Yule-Walker equations. To the extent that the autocovariances are not independently known e.g., from a theory, most estimation algorithms in practice resort to forms of least-squares. Note that vectors generated from white noise sequences are orthogonal. The Kolmogoroff-Wiener-Levinson-... approach is recovered by letting $L \to \infty$, that is, the theory assumes the infinite past is known, while practice copes with a finite observed past.

Suppose $\tilde{\varepsilon}$ fails the white noise test. The obvious remedy would be to try using a second vector, $\boldsymbol{\xi}(t-2)$, in the expansion to remove more of the structure, so that,

$$\left\{\begin{array}{cc} \xi(t-1) & \xi(t-2) \\ \xi(t-2) & \xi(t-3) \\ . & . \\ . & . \\ \xi(t-(L-2)) & \xi(t-(L-1)) \end{array}\right\} \begin{bmatrix} a_1 \\ a_2 \end{bmatrix} + \begin{bmatrix} \varepsilon(t) \\ \varepsilon(t-1) \\ . \\ . \\ \varepsilon(t-(L-3)) \end{bmatrix} = \begin{bmatrix} \xi(t) \\ \xi(t-1) \\ . \\ . \\ \xi(t-(L-3)) \end{bmatrix}, \tag{14}$$

{vector4}

represents an AR(2) process, which in scalar form is,

$$\xi(t) = a_1 \xi(t-1) + a_2 \xi(t-2) + \varepsilon(t). \tag{15}$$

{ar2}

Suppose a satisfactory (acceptable) fit has been found and so that one has estimates, $\tilde{a}_1, \tilde{a}_2$, and $\tilde{\sigma}_\varepsilon^2$. Omitting the tildes, but remembering always that all parameters are estimates, one can consider the one-step ahead prediction problem. In Eq. (15) everything is known at time $t+1$ except $\varepsilon(t+2)$, which has zero-mean. Thus the best prediction is,

$$\tilde{\xi}(t+1) = a_1 \xi(t) + a_2 \xi(t-1) + 0,$$

and whose mean square error would be $\left\langle \varepsilon\left(t+1\right)^{2}\right\rangle = \sigma_{\varepsilon}^{2}$. The two-step ahead prediction would be

$$\tilde{\xi}\left(t+2\right) = a_{1}\tilde{\xi}\left(t+1\right) + a_{2}\xi\left(t\right) + 0$$

and for which the prediction error variance is $\left(a_{1}^{2}+1\right)\sigma_{\varepsilon}^{2}$. This process can be continued indefinitely, the prediction error variance increasing monotonically with the prediction horizon, but never exceeding the variance of $\xi\left(t\right)$ itself: the worst prediction is $\tilde{\xi}\left(t+\tau\right)=0$ and whose expected error is the variance of ξ,

$$\left\langle \xi\left(t'\right)\xi\left(t'\right)\right\rangle = R\left(0\right) = \frac{\sigma_{\varepsilon}^{2}\left(1-a_{2}\right)}{(1-a_{1}^{2}-a_{2}^{2})(1-a_{2})-2a_{1}^{2}a_{2}}.$$

See the references. Alternatively, one can transform $\xi\left(t\right)$ into the MA form as described in the text.

The formal coefficient matrices $\mathbf{E}_1$ or $\mathbf{E}$ involve the observed $\xi\left(t\right)$ and inevitably contain errors. Linear least-squares treats $\mathbf{E}$ as perfectly known, but many methods are available for discussing and remedying the bias and other errors introduced by errors in E, leading to non-linear methods (e.g., Total Least Squares; Van Huffel and Vandewalle, 1991), but which are not discussed here.

Appendix B An Ensemble AR(1)

An artificial AR(1), $x\left(t+1\right) = 0.3x\left(t\right) + \varepsilon\left(t\right)$, was generated for 160 samples (10-times the now available record length). The corresponding MA form has, exactly, $b_j = 0.3^j$, $j = 0, 1, ...$

Thus a_1 is known exactly, as is $\varepsilon\left(t\right)$ (generated using a pseudo-random Gaussian algorithm with variance of 1). The resulting record was then divided into 10 segments each of 16 samples ($i = 1$ to 16), and the resulting system solved for $\tilde{a}_1^{(i)}$ and the estimated $\varepsilon^{(i)}\left(t\right)$. The record variance is $\left\langle \xi\left(r\right)^{2}\right\rangle = \sigma_{\varepsilon}^{2}/\left(1-a_{1}^{2}\right)$. Fig. 19 shows the results of this experiment: The values of the estimated a_i and equivalently the b_i can and do differ substantially from the known exact values and the calculated prediction error, measured either as one-time step ahead, or as the segment record variance, varies by more than a factor of 3 from one realization to the next. They do not vary by an order of magnitude, and so one might interpret any results with the real records (below) as providing an order of magnitude estimate.

The variability of these estimates is known from the textbook discussions to depend upon the magnitude of a_1 (and that in turn depends directly upon the lag one covariance). With $a_1 = 0.3$, only about 9% of the variance from one time step to the next is correlated. Fig. 20 shows similar results for $a_1 = 0.9$ where about 80% of the variance would be so correlated. The coefficients determined from each realization are more stable, but the prediction error (PE) growth (Fig. 21) with time is more rapid because small errors will persist longer, and the variance of $\xi(r)$ is also greater, being proportional to $1/\left(1-a_1^2\right)$.

Appendix C. Vector AR and Singular Value Decomposition

Consider now a generalization whereby $\xi_{i_0}(t)$ is e.g., the MOC at latitude i_0, and one makes the plausible assumption that it is correlated with, and hence predictable from, its L present and past values at several other latitudes, $j=1$ to J (including i_0). As an example, consider a vector AR(2), using only two latitudes, i_0 and j, and one can write e.g.,

$$\xi_{i0}(t) = a_1\xi_{i_0}(t-1) + a_2\xi_{i_0}(t-2) + b_1\xi_j(t-1) + b_2\xi_j(t-2) + \dots + \varepsilon(t),$$

or in matrix-vector form,

$$\begin{bmatrix} \xi_{i0}(t) \\ \xi_{i0}(t-1) \\ \xi_{i0}(t-2) \\ . \\ \xi_{i0}(t-(L-3)) \end{bmatrix} = \tag{16}$$

{vectorar1}

$$\left\{ \begin{matrix} \xi_{i_0}(t-1) & \xi_{i_0}(t-2) & \xi_j(t-1) & \xi_j(t-2) \\ \xi_{i_0}(t-2) & \xi_{i_0}(t-3) & \xi_j(t-2) & \xi_j(t-3) \\ \xi_{i_0}(t-3) & \xi_{i_0}(t-4) & \xi_j(t-3) & \xi_j(t-4) \\ . & . & . & . \\ . & . & . & . \\ \xi_{i_0}(t-(L-2)) & \xi_{i_0}(t-(L-1)) & \xi_j(t-(L-2)) & \xi_j(t-(L-1)) \end{matrix} \right\} \begin{bmatrix} a_1 \\ a_2 \\ b_1 \\ b_2 \end{bmatrix} + \begin{bmatrix} \varepsilon(t) \\ \varepsilon(t-1) \\ \varepsilon(t-3) \\ . \\ . \\ \varepsilon(t-(L-3)) \end{bmatrix}, \tag{17}$$

where j is any other MOC time series at any latitude (or anyother measured variable anywhere). The b_i should not be confused with the MA coefficients used in the text. If the vector AR is order N, and there are J measured time series (including the one being predicted), the equation set (16) has $L-1$ equations in $J(L-1)$ formal unknowns (not counting the $\varepsilon(r)$). Thus an AR(1) using all 111 latitudes at one degree spacing between 30°S and 80°N of estimated MOC would have 111 unknowns in each of the 16 annual mean observations, leaving it greatly underdetermined, with an increasing number of unknowns with any higher order AR.

The singular value decomposition (SVD) can be used to solve such underdetermined problems (e.g., Wunsch, 2006). The coefficient matrix made up of the expansion vectors (the regressors), is written in canonical form as

$$\mathbf{E} = \lambda_1 \mathbf{u}_1 \mathbf{v}_1^T + \lambda_2 \mathbf{u}_2 \mathbf{v}_2^T + ... \lambda_K \mathbf{u}_K \mathbf{v}_K^T, \qquad (18) \quad \texttt{\{svd2\}}$$

where the $\mathbf{u}_i, \mathbf{v}_i$ are the orthonormal singular vectors, and the λ_i are the singular values. $K \leq 15$, is the maximum possible rank of $\mathbf{E}$ here. The $\mathbf{u}_i$ are often known as empirical orthogonal functions (EOFs) and corresponding $\mathbf{v}_i$ are the temporal coefficients. λ_i^2 is the contribution to the squared norm of $\mathbf{E}$.

In the present case, the singular value decomposition shows that $\mathbf{E}$ is formally of full rank, $K = 15$, and at full rank, $\mathbf{E}$ is exactly represented by 15 pairs of orthonormal vectors in Eq. (18). A more plausible estimate of the useful rank is either 9 or 13, depending upon how large the noise is estimated to be. $K = 9$ suggests approximately nine independent pieces of information amongst the 111 latitudinal values of the MOC at a one-year time lag. The SVD solution is,

$$\tilde{\mathbf{x}} = \mathbf{v}_1 \left(\mathbf{u}_1^T \mathbf{y} / \lambda_1 \right) + \mathbf{v}_2 \left(\mathbf{u}_2^T \mathbf{y} / \lambda_2 \right) + ... + \mathbf{v}_K \left(\mathbf{u}_K^T \mathbf{y} / \lambda_K \right), \qquad (19) \quad \texttt{\{svdsol1\}}$$

but results from this approach are not shown here, as they founder on the same too-short record duration.

References

Anderson, D.L.T., Bryan, K., Gill, A.E., Pacanowski, R.C., 1979. Transient-response of the North Atlantic - some model studies. Journal of Geophysical Research-Oceans and Atmospheres 84, 4795-4815.

Bengtsson, L., Hagemann, S., Hodges, K.I., 2004. Can climate trends be calculated from reanalysis data? Journal of Geophysical Research-Atmospheres 109, DOI 10.1029/2004jd004536.

Bingham, R.J., Hughes, C.W., Roussenov, V., Williams, R.G., 2007. Meridional coherence of the North Atlantic meridional overturning circulation. Geophysical Research Letters 34, L23606 DOI10.1029/2007gl031731.

Box, G.E.P., Jenkins, G.M., Reinsel, G.C., 2008. Time Series Analysis : Forecasting And Control, 4th ed. John Wiley, Hoboken, N.J.

Branstator, G., Teng, H.Y., 2010. Two Limits of Initial-Value Decadal Predictability in a CGCM. Journal of Climate 23, 6292-6311.

Bromwich, D.H., Fogt, R.L., Hodges, K.I., Walsh, J.E., 2007. A tropospheric assessment of the ERA-40, NCEP, and JRA-25 global reanalyses in the polar regions. Journal of Geophysical Research-Atmospheres 112, DOI 10.1029/2006jd007859.

Davis, R.E., 1976. Predictability of sea-surface temperature and sea-level pressure anomalies over North Pacific Ocean. Journal of Physical Oceanography 6, 249-266.

Davis, R.E., 1978. Predictability of sea-level pressure anomalies over North Pacific Ocean. Journal of Physical Oceanography 8, 233-246.

Davis, R.E., 1979. Search for short-range climate predictability. Dynamics of Atmospheres and Oceans 3, 485-497.

Deser, C., Alexander, M.A., Xie, S.P., Phillips, A.S., 2010. Sea surface temperature variability: patterns and mechanisms. Annual Review of Marine Science 2, 115-143.

Gebbie, G. and Huybers. P., 2011. How is the ocean filled? Geophysical Research Letters, 38, DOI10.1029/2011GL046769.

Hamilton, J.D., 1994. Time Series Analysis. Princeton Un. Press.

Hannan, E.J., 1970. Multiple Time Series. John Wiley, New York.

Heimbach, P., C. Wunsch, R. M. Ponte, G. Forget, C. Hill and J. Utke, 2011. Timescales and regions of the sensitivity of Atlantic meridional volume and heat transport magnitudes: toward observing system design, Deep-Sea Research-II 58, 1858-1879 2011.

Hurrell J. and Co-authors, 2010. Decadal climate prediciton: opportunities and challenges, in Proceedings of Ocean Obs09: Sustained Ocean Observations and Information for Society, Vol. 2, Hall, J., Harrison, D. E. and D. Stammer, Eds., ESA Publication WPP-306, doi:10.5270/OceanObs09.cwp.45

Kanzow, T., Johnson, H.L., Marshall, D.P., Cunningham, S.A., Hirschi, J.J.M., Mujahid, A., Bryden, H.L., Johns, W.E., 2009. Basinwide integrated volume transports in an eddy-filled ocean. Journal of Physical Oceanography 39, 3091-3110.

Lawson, C.L., Hanson, R.J., 1995. Solving Least Squares Problems. SIAM, Philadelphia.

Ljung, L., 1999. System Identification: Theory for the User, 2nd Ed. Prentice-Hall, Englewood Cliffs, N. J.

Lorbacher, K., Dengg, J., Boning, C.W., Biastoch, A., 2010. Regional patterns of sea level change related to interannual variability and multidecadal trends in the Atlantic meridional overturning circulation. Journal of Climate 23, 4243-4254.

Meehl, G.A., Goddard, L., Murphy, J., and 17 others., 2009. Decadal prediction: Can it be skillful? Bulletin of the American Meteorological Society 90, 1467-+.

Msadek, R., Dixon, K.W., Delworth, T.L., Hurlin, W., 2010. Assessing the predictability of the Atlantic meridional overturning circulation and associated fingerprints. Geophysical Research Letters 37, L19608, DOI10.1029/2010gl044517

Nelles, O., 2001. Nonlinear System Identification: From Classical Approaches to Neural Networks and Fuzzy Models. Springer, Berlin.

Newman, M., 2007. Interannual to Decadal Predictability of Tropical and North Pacific Sea Surface Temperatures. Journal of Climate 20, 2333-2356.

Priestley, M.B., 1982. Spectral Analysis and Time Series. Volume 1: Univariate Series. Volume 2: Multivariate Series, Prediction and Control. Academic, London.

Reynolds, R.W., Smith, T.M., 1995. A high-resolution global sea-surface temperature climatology. Journal of Climate 8, 1571-1583.

Robinson, E.A., 1981. Time Series Analysis And Applications. Goose Pond Press, Houston, Tex.

Rossby, T., Flagg, C.N., Donohue, K., 2005. Interannual variations in upper-ocean transport by the Gulf Stream and adjacent waters between New Jersey and Bermuda. Journal of Marine Research 63, 203-226.

Rossby, T., Flagg, C.N., Donohue, K., 2010. On the variability of Gulf Stream transport from seasonal to decadal timescales. Journal of Marine Research, 68, 503-522.

Storch, H.v., Zwiers, F.W., 2001. Statistical Analysis In Climate Research, 1st pbk. ed. Cambridge University Press.

Tizard, T.H., Mosely, H.N., Buchanan, J.Y., Murray, J., 1885. Report on the Scientific Results of the Voyage of H. M. S. Challenger During the Years 1873-1876, Narrative of the Cruise of H. M. S. Challenger with a General Account of the Scientific Results of the Expedition, 1, First Part. H. M. Stationery Office, Edinburgh.

Tourre, Y.M., Rajagopalan, B., Kushnir, Y., 1999. Dominant patterns of climate variability in the Atlantic Ocean during the last 136 years. Journal of Climate 12, 2285-2299.

Van Huffel, S., Vandewalle, J., 1991. The Total Least Squares Problem. Computational Aspects and Analysis. SIAM, Philadelphia.

Veronis, G., Stommel, H., 1956. The action of variable wind stresses on a stratified ocean. Journal of Marine Research, 15, 43-75.

Vinogradova, N.T., Ponte, R.M., and Heimbach, P., 2010: Dynamics and forcing of sea surface temperature variability on climate time scales. Journal of Climate, submitted.

Wang, W.Q., Kohl, A., Stammer, D., 2010. Estimates of global ocean volume transports during 1960 through 2001. Geophysical Research Letters 37.

Woollings, T., Hoskins, B., Blackburn, M., Hassell, D., Hodges, K., 2010. Storm track sensitivity to sea surface temperature resolution in a regional atmosphere model. Climate Dynamics 35, 341-353.

Wunsch, C., 1999. The interpretation of short climate records, with comments on the North Atlantic and Southern Oscillations. Bulletin of the American Meteorological Society 80, 245-255.

Wunsch, C., 2006. Discrete Inverse And State Estimation Problems: With Geophysical Fluid Applications. Cambridge University Press.

Wunsch, C., 2008. Mass and volume transport variability in an eddy-filled ocean. Nature Geoscience 1, 165-168.

Wunsch, C., Heimbach, P., 2006. Estimated decadal changes in the North Atlantic meridional overturning circulation and heat flux 1993-2004. Journal of Physical Oceanography 36, 2012-2024.

Wunsch, C., Heimbach, P., 2007. Practical global oceanic state estimation. Physica D-Nonlinear Phenomena 230, 197-208.

Wunsch, C., Heimbach, P., 2009. The global zonally integrated ocean circulation, 1992-2006: seasonal and decadal variability. Journal of Physical Oceanography 39, 351-368.

Wunsch, C., Heimbach, P., Ponte, R.M., Fukumori, I., Members, E.-G.C., 2009. The global general circulation of the ocean estimated by the ECCO-consortium. Oceanography 22, 88-103.

Yin, J.J., Schlesinger, M.E., Stouffer, R.J., 2009. Model projections of rapid sea-level rise on the northeast coast of the United States. Nature Geoscience 2, 262-266.

Zanna, L., Heimbach, P., Moore, A.M., Tziperman, E., 2011. Optimal excitation of interannual Atlantic meridional overturning circulation variability. Journal of Climate 24, 413-427.

Zhang, H.H., Wu, L.X., 2010. Predicting North Atlantic sea surface temperature variability on the basis of the first-mode baroclinic Rossby wave model. Journal of Geophysical Research-Oceans 115, C09030, DOI10.1029/2009jc006017.

Figure and Table Captions

Table 1. Summary statistics. Variances are either in $^{\circ}C^2$(for SST) or Sv^2 for the meridional overturning circulation (MOC). PE is the prediction error. The record variance is not the sum of the component variances because the monthly values include the low frequency variability. Some prediction error values are omitted as being of no particular interest. GBB denotes the Grand Bahama Bank square, and ECCO is the consortium Estimating the Circulation and Climate of the Ocean. MA(M) indicates that the prediction error was deduced by converting the AR(1) model into an MA of order M.}

Fig. 1. Sixteen year time mean sea surface temperature (SST, in °C) from the ECCO-GODAE estimate in the North Atlantic. Small white square, called the Grand Banks Box—GBB, is used as protypical of the areal prediction problem.

2. The Grand Banks Box (GBB) area average temperature, $T_G(t)$ (solid curve), the best-fitting annual cycle including its first three harmonics (dashed), and the monthly residuals of the annual cycle (dotted). Start is 1992.

3. (a) Periodogram of $T_G(t)$ for the ECCO estimate (dashed) and longer Reynolds and Smith (1995) time series (solid curve). (b) Cumulative integral of the periodgrams in (a) normalized to a sum of 1, so that the dominance by the annual peak in both cases is clear. (c) Spectral estimates for both time series after removal of the annual cycle and its harmonics. The annual peak is so narrow as to be indistinguishable at this resolution from a pure sinusoid. At low frequencies, a power law of frequency to the power -2.5 is approximately correct.

4. Monthly values of $T'_{GBB}(t)$, (start is 1992) residual of the area average GBB SST, after removal of the annual cycle and its harmonics. The visual trend, if secular—meaning extending far beyond the record length—contributes to the apparent predictability as it is here treated as part of a red noise process. (Repeated from Fig. 2.)

5. Prediction error out to 6 months for $T'_{GBB}(t)$. Note that the variance of the monthly means of $T'_{GBB}(t)$ is $0.7^{\circ}C^2$, which is the maximum prediction

6. Annual mean values for the Reynolds and Smith (1995)—solid line and the ECCO results in the GBB (dashed).

7. Prediction error growth in *years* for $T'_{GBB}(t)$ from an AR(1) converted to an MA(5). Total variance is 0.78°C.

8. Zonal and time mean meridional transport (not the stream function). The upper 200m has a particularly complex structure at low latitudes (see Wunsch and Heimbach, 2009).

9. The maximum meridional transport, integrated from the sea surface, averaged over 16 years (upper panel). Lower panel shows the depth where the time-mean value is obtained.

10. Monthly values of $V(y, z, t)$ in Sverdrups ($10^6 \mathrm{m}^3/\mathrm{s}$) for a succession of Januarys showing the typical interannual variability occurring at depth. Year 2 is 1993. The origin of these small meridional scale features is not explored here, but may be associated with response to the Ekman forcing in shallow water areas (e.g., Davis, 2010).

11. The monthly MOC *anomaly* without the annual mean cycle at 25°N and 50°N (a) and at 20°S (b). Little visual similarity is apparent.

12. MOC variances (solid curve), the annual contribution (with harmonics) as a function of latitude in Sv^2 (dashed line), and the residual after removal of the annual cycle (dotted).

13. Power density spectral estimate of monthly MOC values at three latitudes. The annual cycle and its harmonics are visible, as is the low frequency asymptote toward white noise behavior. This spectral density is, overall, nearly flat. The annual peak is broadened by the multi-tapers used to form the estimated spectrum and the very lowest frequency estimate has a known negative bias.

14. Correlation matrix with latitude of the annual mean MOC (left panel). Right panel is an expanded color scale version of the left panel, showing only the apparently statistically significant values. No negative correlations are significant.

15. Coherence amplitude and phase between 20.5°N and 50.5°N. Significant coherence vanishes at periods longer than one year. High frequency coherence is in large part that of the annual cycle and its harmonics and for which the level-of-no-significance shown is inappropriate.

16. Coherence between the monthly MOC at 20.5°S and 50.5°N. Apart from the annual cycle, where the conventional statistics do not apply, there is no significant coherence.

17. Prediction error of the MOC as a function of year at 50°N from a univariate AR(1).

18. Correlation coefficient between the maximum MOC through time (annual means) with the GBB SST (left panel). The last row and column are the SST correlations. Omitting the last row and column repeats the values in Fig. 14. Right panel shows the same results

but with a linear trend removed from SST, thus reducing the correlations. No values below magnitude 0.5 are statistically significant. (These correlations are with the MOC defined as integrated to the time-mean maximum depth. Results with the time-varying integration depth are indistinguishable.)

19. $\tilde{a}^{(i)}$ from each 16-element segment of the record in Fig. 19 (a) panel; true value is $a = 0.3$; (b) the estimated uncertainty in those values and (c) the variance in the 15 samples estimates of $\varepsilon(t)$ in the segment. The correct value is 1.

20. Same as Fig. 19 except for $a = 0.9$.

21. The 10 different realizations of the estimated MA coefficients for $a = 0.9$ (left panel), and the corresponding prediction error growth through time (right panel). Each line corresponds to a different 16 time step realization. True values are shown as 'o'.

Variable	GBB SST (ECCO) $^{\circ}C^2$	GBB (Reynolds & Smith) $^{\circ}C^2$	MOC at 20°S Sv^2	MOC at 25°N Sv^2	MOC at 50°N Sv^2
Total Record	10.2	9.9	6.5	10.2	10.5
Annual cycle	9.45 (93%)	8.8	2.1	2.9	3.6
Record w/o annual cycle	0.78	0.7 (7%)	4.4	7.2	7.0
Annual averages	0.50 (5% of the total)	0.36(3.6%)	1.9	2.2	1.8
One month PE	0.2	0.3 (MA(3) and MA(10))	2.4 MA(4)	6.5 MA(4)	5.6 MA(4)
Six month PE	0.6	0.7	-	-	-
One year PE	0.2 (AR(1) with trend)	0.05 (MA(4))	0.5 MA(4)	0.2 MA(4)	0.8 MA(4)
Three year PE	0.4	0.3	-	-	1.5

Table 1: Summary statistics. Variances are either in $^{o}C^2$ (for SST) or Sv^2 for the meridional overturning circulation (MOC). PE is the prediction error. The record variance is not the sum of the component variances because the monthly values include the low frequency variability. Some prediction error values are omitted as being of no particular interest. GBB denotes the Grand Bahama Bank square, and ECCO is the consortium Estimating the Circulation and Climate of the Ocean. MA(M) indicates that the prediction error was deduced by converting the AR(1) model into an MA of order M. {TableKey}

{table}

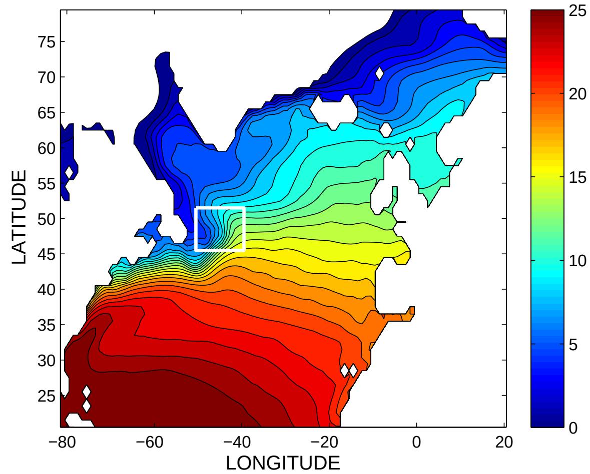

Figure 1: Sixteen year time mean sea surface temperature (SST, in °C) from the ECCO-GODAE estimate in the North Atlantic. Small white square, called the Grand Banks Box—GBB, is used as protypical of the areal prediction problem. {sst_time_mean

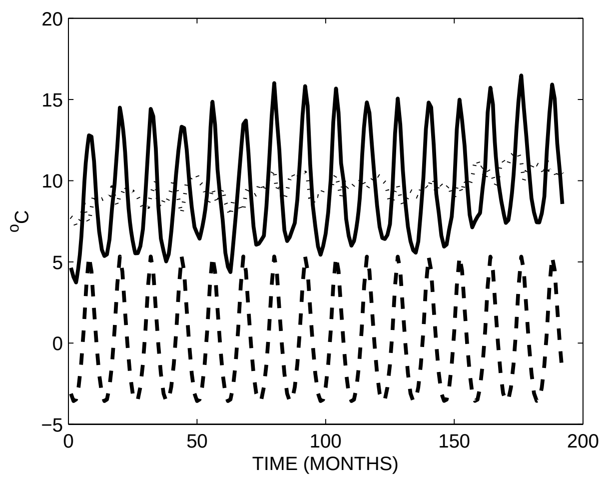

Figure 2: The Grand Banks Box (GBB) area average temperature $T_G(t)$ (solid curve), the best-fitting annual cycle including its first three harmonics (dashed), and the monthly residuals of the annual cycle (dotted). Start is 1992. {sst_areaavg&r

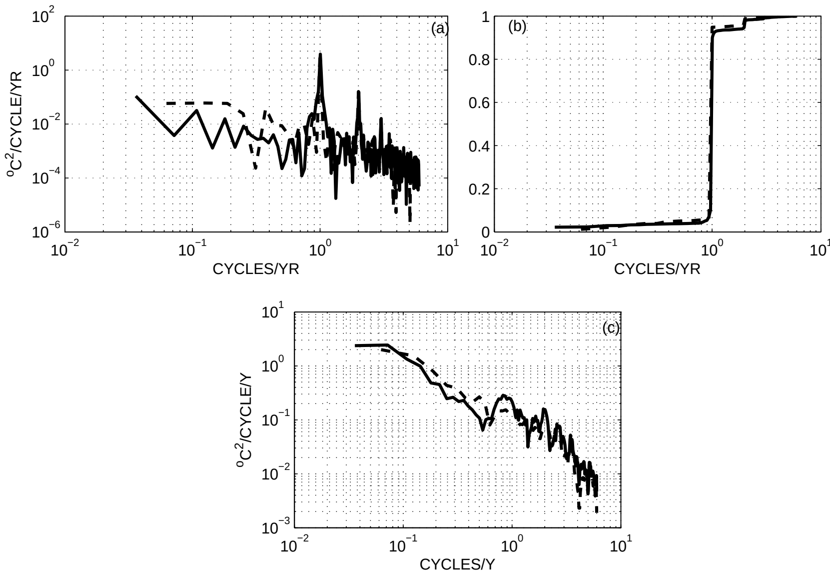

Figure 3: (a) Periodogram of $T_G(t)$ for the ECCO estimate (dashed) and longer Reynolds and Smith (1995) time series (solid curve). (b) Cumulative integral of the periodgrams in (a) normalized to a sum of 1, so that the dominance by the annual peak in both cases is clear. (c) Spectral estimates for both time series after removal of the annual cycle and its harmonics. The annual peak is so narrow as to be indistinguishable at this resolution from a pure sinusoid. At low frequencies, a power law of frequency to the power -2.5 is approximately correct. {area_periodo_

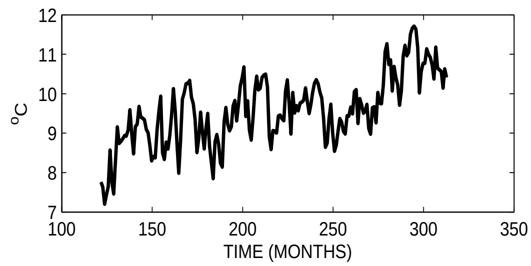

Figure 4: Monthly values of $T'_{GBB}(t)$, (start is 1992) residual of the area average GBB SST, after removal of the annual cycle and its harmonics. The visual trend, if secular—meaning extending far beyond the record length—contributes to the apparent predictability as it is here treated as part of a red noise process. (Repeated from Fig. 2.) {sst_area_noan

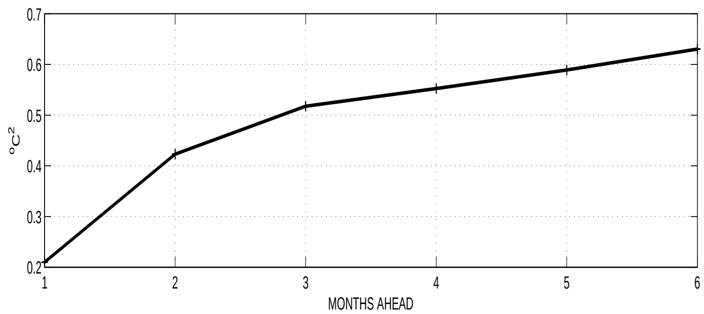

Figure 5: Prediction error out to 6 months for $T'_{GBB}(t)$. Note that the variance of the monthly means of $T'_{GBB}(t)$ is $0.7°\mathrm{C}^2$, which is the maximum prediction error.

{gbb_pe_ma6.ep

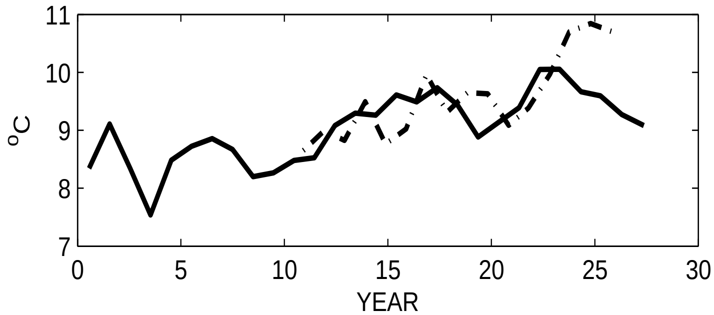

Figure 6: Annua ECCO results in
the GBB (dashed

{area_annmeans

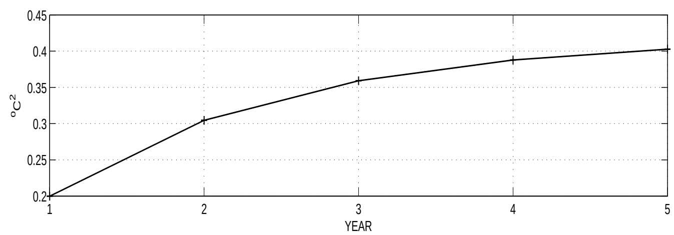

Figure 7: Prediction error growth in *years* for $T'_{GBB}(t)$ from an AR(1) converted to an MA(5). Total variance is 0.78°C.

{pred_error_ar

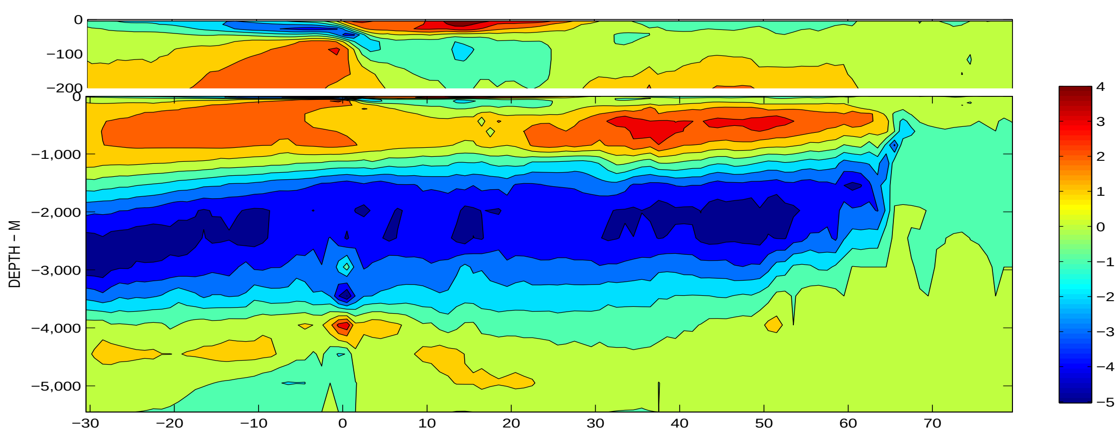

Figure 8: Zonal and time mean meridional transport (not the stream function). The upper 200m has a particularly complex structure at low latitudes (see Wunsch and Heimbach, 2009).

{moc_timemean_

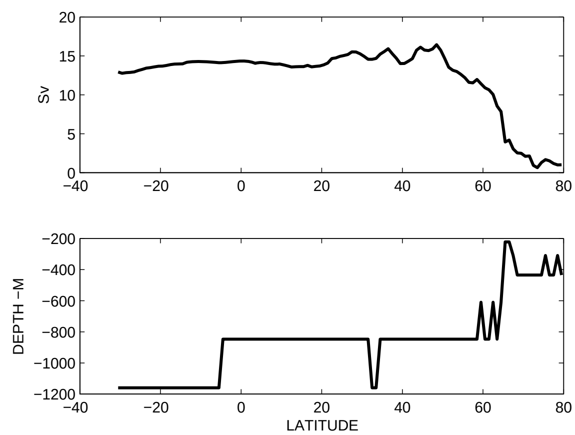

Figure 9: The maximum meridional transport, integrated from the sea surface, averaged over 16 years (upper panel). Lower panel shows the depth where the time-mean value is obtained. {mocmax&deptht

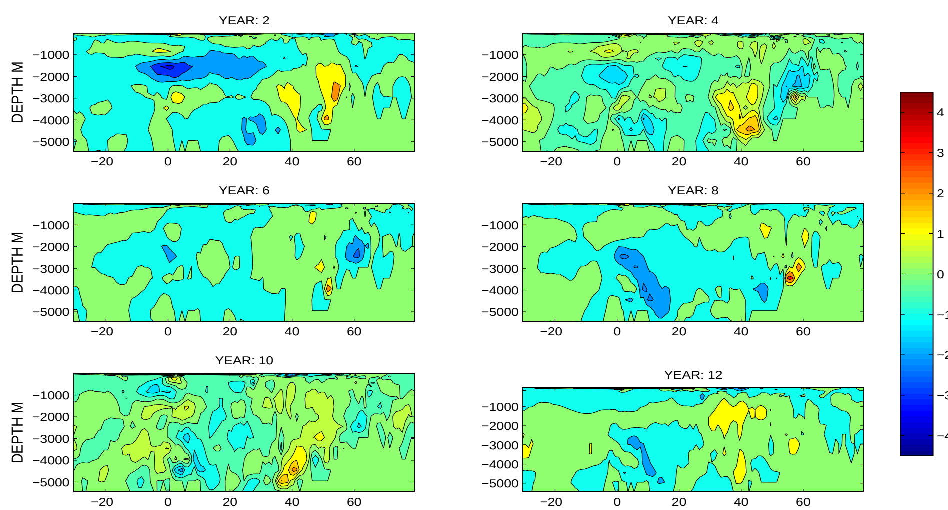

Figure 10: Monthly values of $V(y,z,t)$ in Sverdrups ($10^6\mathrm{m}^3/\mathrm{s}$) for a succession of Januarys showing the typical interannual variability occurring at depth. Year 2 is 1993. The origin of these small meridional scale features is not explored here, but may be associated with response to the Ekman forcing in shallow water areas (e.g., Davis, 2010). {moc_every2yea

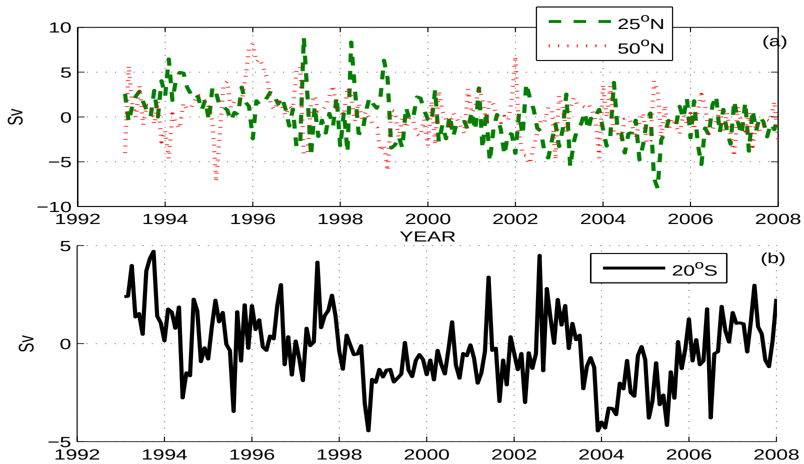

Figure 11: The maximum monthly MOC *anomaly* without the annual mean cycle at 25°N and 50°N (a) and at 20°S (b). Little visual similarity is apparent. {moc_3lats_ts_

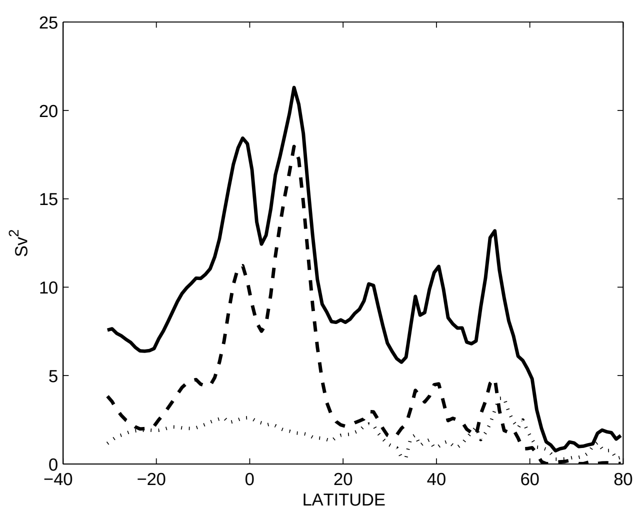

Figure 12: MOC variances (solid curve), the annual contribution (with harmonics) as a function of latitude in Sv^2 (dashed line), and the residual after removal of the annual cycle (dotted). {var_all_lats&

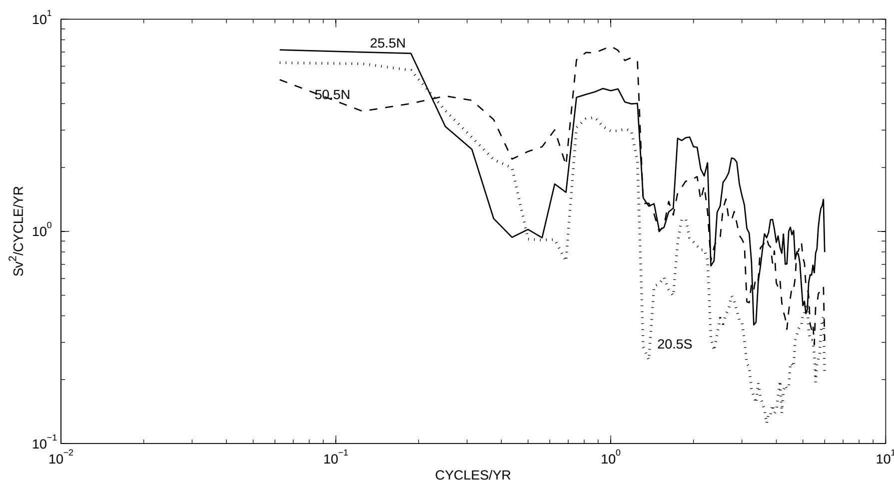

Figure 13: Power density spectral estimate of monthly MOC values at three latitudes. The annual cycle and its harmonics are visible, as is the low frequency asymptote toward white noise behavior. This spectral density is, overall, nearly flat. The annual peak is broadened by the multi-tapers used to form the estimated spectrum and the very lowest frequency estimate has a known negative bias. {moc_pd_3lats.

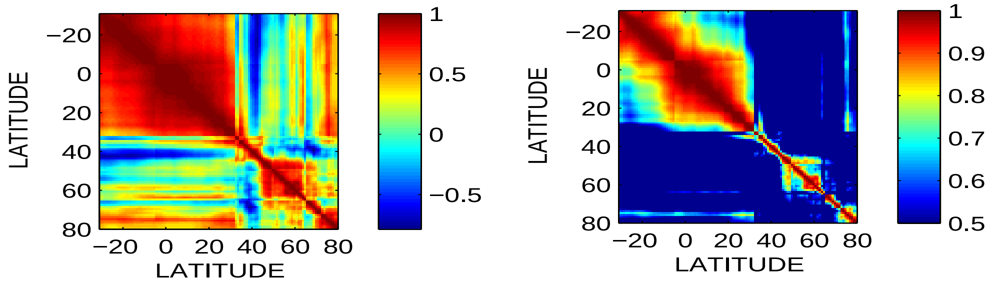

Figure 14: Correlation matrix with latitude of the annual mean MOC (left panel). Right panel is an expanded color scale version of the left panel, showing only the apparently statistically significant values. No negative correlations are significant.

{moc_latcorr_a

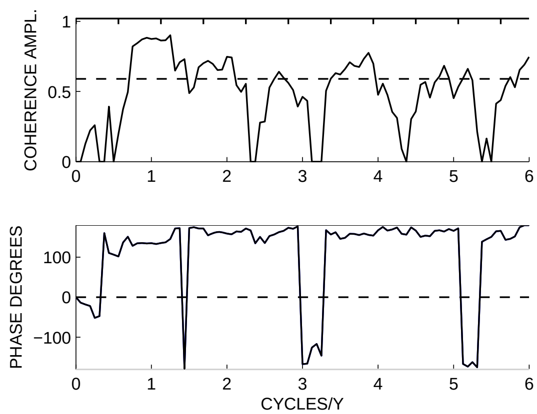

Figure 15: Coherence amplitude and phase between 20.5°N and 50.5°N. Significant coherence vanishes at periods longer than one year. High frequency coherence is in large part that of the annual cycle and its harmonics and for which the level-of-no-significance shown is inappropriate. {moc_coher25n5

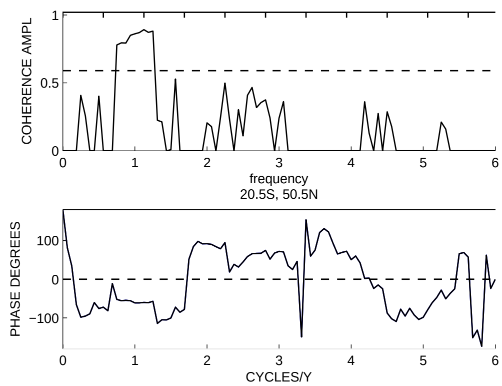

Figure 16: Coherence between the monthly MOC at 20.5°S and 50.5°N. Apart from the annual cycle, where the conventional statistics do not apply, there is no significant coherence. {moc_coher21s5

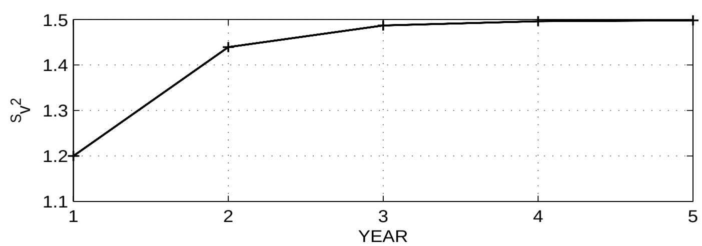

Figure 17: Prediction error as a function of year at 50°N from a univariate AR(1). {pemoc50nfroma

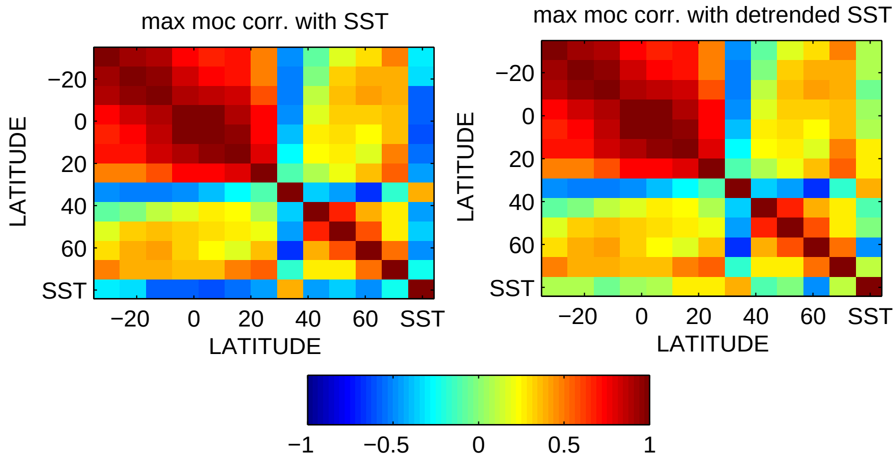

Figure 18: Correlation coefficient between the maximum MOC through time (annual means) with the GBB SST (left panel). The last row and column are the SST correlations. Omitting the last row and column repeats the values in Fig. 14. Right panel shows the same results but with a linear trend removed from SST, thus reducing the correlations. No values below magnitude 0.5 are statistically significant. (These correlations are with the MOC defined as integrated to the time-mean maximum depth. Results with the time-varying integration depth are indistinguishable.) {mocmax_latcor

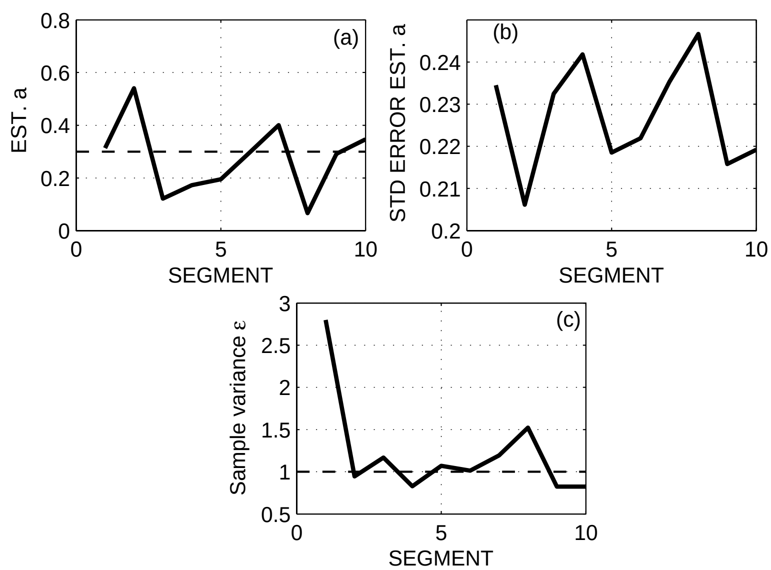

Figure 19: $\tilde{a}^{(i)}$ from each 16-element segment of the record in Fig. 19 (a) panel; true value is $a = 0.3$; (b) the estimated uncertainty in those values and (c) the variance in the 15 samples estimates of $\varepsilon(t)$ in the segment. The correct value is 1.

{atrue3sols.ep

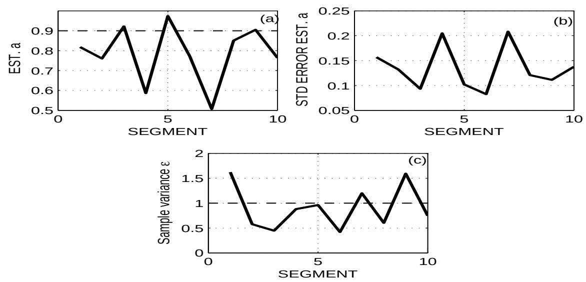

Figure 20: Same as Fig. 19 except for $a = 0.9$. {atrue9sols.ep

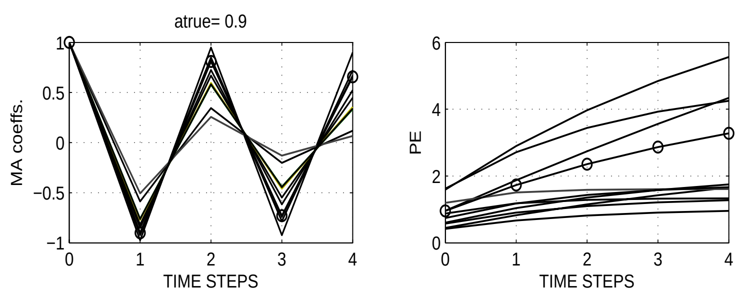

Figure 21: The 10 different realizations of the estimated MA coefficients for $a = 0.9$ (left panel), and the corresponding prediction error growth through time (right panel). Each line corresponds to a different 16 time step realization. True values are shown as 'o'. {atrue9ma&pe.e